

Adaptive Interval Type-2 Fuzzy Sliding Mode Controller Design for Flexible Air-breathing Hypersonic Vehicles

Junlong Gao, Ruyi Yuan, and Jianqiang Yi

Institute of Automation
Chinese Academy of Sciences
Beijing 100190, China

{junlong.gao, ruyi.yuan, jianqiang.yi}@ia.ac.cn

Chengdong Li

School of Information and Electrical Engineering
Shandong Jianzhu University
Jinan 250101, China
lichengdong@sdu.edu.cn

Abstract—In this paper an adaptive interval type-2 fuzzy sliding mode controller, which is applied to flexible air-breathing hypersonic vehicle (FAHV) longitudinal model, is designed based on interval type-2 fuzzy logic systems (IT2-FLS) and sliding mode control (SMC) theory. In order to get FAHV longitudinal model stably controlled, we decouple the model into velocity and altitude channels through output feedback linearization. Moreover, due to the severe uncertainties which mainly come from unpredictable varying aerodynamic interferences and mutual couplings in airframe flexible modes and those difficulties of computing nonlinear functions with high-order derivatives under practical conditions, we design a sliding mode controller to achieve system convergence and adopt IT2-FLS to estimate the nonlinear functions with bounded parameter uncertainties online for counteracting the tracking errors and suppressing flexible vibrations. The adaptive law of interval type-2 fuzzy sliding mode controller is derived through Lyapunov synthesis approach. Furthermore, we adopt tracking differentiator (TD) and nonlinear state observer (NSO) algorithms to generate the real-time derivatives and high-order approximate commands in velocity and altitude channels, respectively. Several comparisons have been done in this paper and the simulation results validate the robustness and effectiveness of the proposed controller.

Keywords—Interval Type-2 Fuzzy Logic System; Sliding Mode Control; State Observer; Flexible Air-breathing Hypersonic Vehicle

I. INTRODUCTION

Hypersonic vehicles particularly refer to those aerial or aerospace vehicles which can reach over 5 Mach, with high payload capacity and reusability. They are widely studied since 1960s not only because of the bright prospects in both civil and military applications, but also for the challenging tasks in aerodynamics, control systems and so forth. To date, outstanding fundamental works have been done on the generic hypersonic flight vehicles (GHFV) [1]. The research focus now is on the branch of air-breathing hypersonic vehicles (AHV). Though some achievements have been completed such as the research of scramjet engine and successful tests of the wave-rider shape vehicles X-43A and X-51A [2, 3], AHV

still has a lot of works to be done before practical applications. Recently, the flexible air-breathing hypersonic vehicle (FAHV) which reflects flexible modes of AHV model has been studied for the noticeable flexibility effects, uncertainties and disturbances. These effects may cause negative impacts on flight safety and lead those aforementioned advantages of hypersonic vehicles into fantastic but meaningless concepts. To address these issues, one of the research focuses is how to deal with flexible modes and so on in control system design and relevant works.

Sliding mode control (SMC) is one of the control techniques, which shows high robustness especially in nonlinear system applications and is the most common control technique in realistic applications other than PID control. However, the shortage of SMC is the control trajectory may appear chattering effects which make negative contributions to system robustness and are not expected in control. In order to suppress the chattering, one way is to use high-order sliding mode [4] and the other ways include improvements of the sliding surface structures, optimizations and hybrid techniques with other control strategies [5] such as neural networks, fuzzy logic systems, etc.

Fuzzy logic is being widely studied for its unique linguistic descriptions. The foundation of fuzzy logic is type-1 and type-2 fuzzy sets (T1 & T2-FSs) which were separately introduced by Zadeh in 1965 and 1975 [6], whereas type-2 fuzzy set is the extension of type-1 fuzzy set with another type of membership functions (MFs). A sample of T2-FS membership function is visibly shown in Fig.1 a), the higher curve is called upper MF (UMF) and the curve beneath UMF is called lower MF (LMF). The banded region between UMF and LMF is named footprint of uncertainty (FOU). FOU adds another degree of freedom in MF, making T2-FS more capable to deal with uncertainties than T1-FS. The structure of type-2 fuzzy logic system (T2-FLS) is shown in Fig.1 b). The “Type reducer” transforms the inference engine output from T2-FS into T1-FS before the final defuzzification. Interval type-2 fuzzy logic systems (IT2-FLS) are widely researched

This work is supported by National Nature Science Foundation of China under grant No. 61273149, No. 61403381, No. 61421004 and No. 61473176.

and used into applications for their simpler structure and lower computational cost than general type-2 FLS [7].

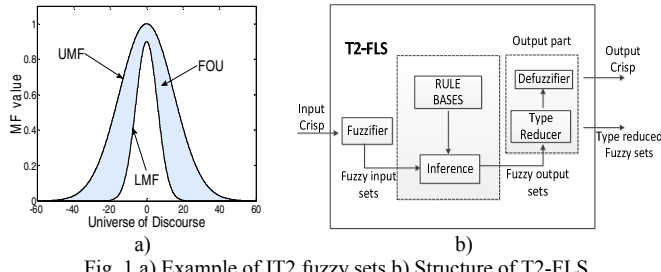


Fig. 1 a) Example of IT2 fuzzy sets b) Structure of T2-FLS

Since fuzzy sliding mode control has already been proposed for decades, type-2 or interval type-2 fuzzy sliding mode control has shown the combinations of both T2-FLS and SMC advantages, which is not only more capable of handling uncertainties or disturbances but also can dramatically reduce the number of rules [8]. Moreover, interval type-2 fuzzy sliding mode control has been proposed by theoretical studies and applied in those systems with high nonlinearities and uncertainties, e.g. chaotic systems [9].

In summary, this paper proposes an adaptive interval type-2 fuzzy sliding mode controller (IT2-FSMC) for FAHV. We design a sliding mode controller as the basic controller to achieve system convergence based on feedback linearization of FAHV longitudinal model. Interval type-2 fuzzy logic system is used to estimate the nonlinear time-varying function values with uncertainties to compensate the sliding mode controller, the designed adaptive law through Lyapunov synthesis approach is used to optimize the IT2-FSMC. Step signals in both velocity and altitude channels are used to verify the robustness and effectiveness of the adaptive IT2-FSMC. Moreover, comparative simulations with different uncertainty levels validate high robustness and effectiveness of the controller.

The rest of this paper is organized as follows: Section 2 describes the longitudinal model of FAHV; Section 3 provides the detail control design procedures of the adaptive IT2-FSMC; Section 4 provides the proof of the adaptive law and analysis of the system stability; Section 5 gives simulations in different level of parameter uncertainties; Section 6 draws conclusions.

II. PRELIMINARIES

A. FAHV Model Description

Among the three unveiled FAHV simplified models [10-13], we choose the one which illustrates the flexibility effects as a free-free beam so that the flexible modes can be reflected through forces and moments.

The nonlinear longitudinal dynamic motion equations of the FAHV are given as:

$$\dot{V} = (T \cos \alpha - D) / m - g \sin \gamma \quad (1)$$

$$\dot{\gamma} = (L + T \sin \alpha) / (mV) - g \cos \gamma / V \quad (2)$$

$$h = V \sin \gamma \quad (3)$$

$$\dot{\alpha} = q - \dot{\gamma} \quad (4)$$

$$\dot{q} = M_{yy} / I_{yy} \quad (5)$$

$$\ddot{\eta}_i = -2\xi_i \omega_i \dot{\eta}_i - \omega_i^2 \eta_i + N_i, \quad i = 1, 2, 3 \quad (6)$$

Eleven flight states are composed in this model, where $[V, \gamma, h, \alpha, q]$ and $\boldsymbol{\eta} = [\eta_1, \dot{\eta}_1, \eta_2, \dot{\eta}_2, \eta_3, \dot{\eta}_3]$ represents rigid-body states and the first three flexible modes, respectively. Moreover, V, γ, h, α, q stand for the vehicle speed, flight path angle, altitude, angle of attack and pitch rate separately. The mode frequencies which can cause the flexible-mode to generate severe mode vibrations are set as $\omega_1 = 21.17 \text{ rad/s}$, $\omega_2 = 53.92 \text{ rad/s}$ and $\omega_3 = 109.1 \text{ rad/s}$ with the damping ratio constant $\xi_i = 0.02$. The canard deflection δ_c and elevator deflection δ_e are ganged together. Their relationship is presented through the canard deflection gain k_{ec} as: $\delta_c = k_{ec} \delta_e$, $k_{ec} = -C_L^{\delta_e} / C_L^{\delta_c}$. Coefficients which determine the thrust T , drag D , lift L , pitching moment M and generalized forces N_i are given below [14]:

$$\begin{cases} L \approx 0.5\rho V^2 s C_L(\alpha, \boldsymbol{\delta}, \boldsymbol{\eta}) & D \approx 0.5\rho V^2 s C_D(\alpha, \boldsymbol{\delta}, \boldsymbol{\eta}) \\ T \approx 0.5\rho V^2 s [C_{T,\phi}(\alpha)\phi + C_T(\alpha) + C_T^\eta \boldsymbol{\eta}] & \\ M_{yy} \approx z_T T + 0.5\rho V^2 s \bar{c} C_M(\alpha, \boldsymbol{\delta}, \boldsymbol{\eta}) & \\ N_i \approx 0.5\rho V^2 s [N_i^{\alpha^2} \alpha^2 + N_i^\alpha \alpha + N_i^{\delta_e} \delta_e + N_i^{\delta_c} \delta_c + N_i^0 + N_i^\eta \boldsymbol{\eta}] & \end{cases} \quad (7)$$

$$\begin{cases} C_{T,\phi}(\alpha) = C_T^{\phi\alpha^3} \alpha^3 + C_T^{\phi\alpha^2} \alpha^2 + C_T^{\phi\alpha} \alpha + C_T^0 \\ C_T(\alpha) = C_T^3 \alpha^3 + C_T^2 \alpha^2 + C_T^1 \alpha + C_T^0 \\ C_L(\alpha, \boldsymbol{\delta}, \boldsymbol{\eta}) = C_L^\alpha \alpha + C_L^{\delta_e} \delta_e + C_L^{\delta_c} \delta_c + C_L^0 + C_L^\eta \boldsymbol{\eta} \\ C_D(\alpha, \boldsymbol{\delta}, \boldsymbol{\eta}) = C_D^{\alpha^2} \alpha^2 + C_D^\alpha \alpha + C_D^{\delta_e^2} \delta_e^2 + C_D^{\delta_c^2} \delta_c^2 + C_D^{\delta_e} \delta_e + C_D^{\delta_c} \delta_c + C_D^0 + C_D^\eta \boldsymbol{\eta} \end{cases} \quad (8)$$

$$C_M(\alpha, \boldsymbol{\delta}, \boldsymbol{\eta}) = C_M^{\alpha^2} \alpha^2 + C_M^\alpha \alpha + C_M^{\delta_e} \delta_e + C_M^{\delta_c} \delta_c + C_M^0 + C_M^\eta \boldsymbol{\eta}$$

$$\boldsymbol{C}_j^\eta = [C_j^{\eta_1} \ 0 \ C_j^{\eta_2} \ 0 \ C_j^{\eta_3} \ 0], \quad j = T, L, D, M$$

$$\boldsymbol{N}_i^\eta = [N_i^{\eta_1} \ 0 \ N_i^{\eta_2} \ 0 \ N_i^{\eta_3} \ 0], \quad i = 1, 2, 3$$

where $\boldsymbol{\delta} = [\delta_c, \delta_e]^T$, the air density ρ is defined as $\rho = \rho_0 \exp(-h/h_0)$ with $\rho_0 = 6.7429 \times 10^{-5} \text{ Slug/ft}^3$ and $h_0 = 24000 \text{ ft}$. A second-order engine model is introduced as :

$$\ddot{\phi} = -2\xi_n \omega_n \dot{\phi} - \omega_n^2 \phi + \omega_n^2 \phi \quad (9)$$

where ξ_n is the engine damping ratio, ω_n is the nominal engine frequency. The actuator-limitations are set as:

$$\delta_e, \delta_c \in [-20^\circ, 20^\circ], \phi \in [0.05, 1.5] \quad (10)$$

The output vector is chosen as $\mathbf{y} = [V, h]^T$.

III. CONTROL DESIGN

In order to reduce the adverse impacts of the uncertainties which may occur in FAHV longitudinal model both in flexible dynamics and unknown interferences, we design an adaptive interval type-2 fuzzy sliding mode controller. In this section,

we give design details including FAHV feedback linearization, controller design processes and the algorithms to obtain high-order derivatives of commands and feedback signals. The overall control system can be seen in Fig. 2.

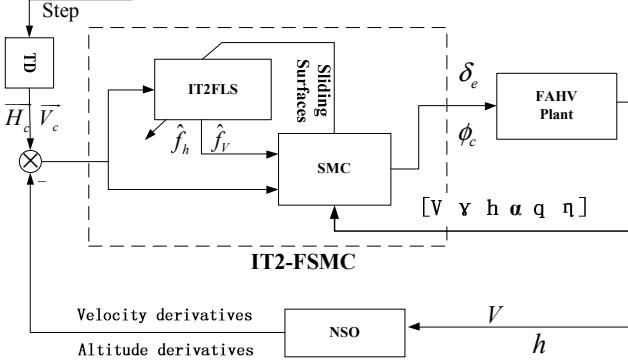


Fig. 2 Diagram of the Overall Control System

A. Sliding Surface Design

In the control scheme, we use the elevator deflection δ_e and throttle setting value ϕ_c as the control vector \mathbf{u} to make the FAHV flight control system track the reference signal vector $[v_c, h_c]^T$, which means the system should make the tracking error $[e_v, e_h]^T$ converge to zero. Therefore, we define the sliding surfaces as:

$$S_1 = (d/dt + \lambda_1)^3 \int_0^t e_v dt \quad (11)$$

$$S_2 = (d/dt + \lambda_2)^4 \int_0^t e_h dt \quad (12)$$

where $e_v = v - v_c$, $e_h = h - h_c$. v, v_c, h, h_c are real-time signals and command signals in velocity and altitude, respectively.

B. Feedback Linearization of FAHV

For sake of full state feedback from FAHV nonlinear dynamics to global linearization, we calculate the first derivative of (11) and (12) respectively and get equations which include $\ddot{v}, \ddot{v}_c, h^{(4)}, h_c^{(4)}$ based on differential geometric control theory [15]. We obtain the following expressions:

$$\begin{cases} \dot{S}_1 = -\ddot{V}_c + f_v + 3\lambda_1 \dot{e}_v + 3\lambda_1^2 \dot{e}_v + \lambda_1^3 e_v + G_{11} \delta_e + G_{12} \phi_c \\ \dot{S}_2 = -h_c^{(4)} + f_h + 4\lambda_2 \ddot{e}_h + 6\lambda_2^2 \dot{e}_h + 6\lambda_2^3 e_h + \lambda_2^4 e_h + G_{21} \delta_e + G_{22} \phi_c \end{cases} \quad (13)$$

where

$$f_v = (\omega_1 \cdot \ddot{\mathbf{x}}_0 + \dot{\mathbf{x}}^T \cdot \boldsymbol{\Omega}_2 \cdot \dot{\mathbf{x}}) / m \quad (14)$$

$$\begin{aligned} f_h &= 3\ddot{V} \cdot \dot{\gamma} \cdot \cos \gamma - 3\dot{V} \cdot \dot{\gamma}^2 \cdot \sin \gamma + 3\dot{V} \cdot \dot{\gamma} \cdot \cos \gamma - \\ &\quad 3V \cdot \dot{\gamma} \cdot \dot{\gamma} \cdot \sin \gamma - V \cdot \dot{\gamma}^3 \cdot \cos \gamma + \\ &\quad (\omega_1 \cdot \ddot{\mathbf{x}}_0 + \dot{\mathbf{x}}^T \cdot \boldsymbol{\Omega}_2 \cdot \dot{\mathbf{x}}) \cdot \sin \gamma / m + \end{aligned} \quad (15)$$

$$V \cdot (\boldsymbol{\pi}_1 \cdot \ddot{\mathbf{x}}_0 + \dot{\mathbf{x}}^T \cdot \boldsymbol{\Pi}_2 \cdot \dot{\mathbf{x}}) \cdot \cos \gamma$$

$$G_{11} = \left(c_e \rho V^2 Sc / 2m \cdot I_{yy} \right) \left(C_M^{\delta_e} - C_L^{\delta_e} C_M^{\delta_c} / C_L^{\delta_c} \right) \quad (16)$$

$$((\partial T / \partial \alpha) \cos \alpha - T \cdot \sin \alpha - \partial D / \partial \alpha)$$

$$G_{12} = (\partial T / \partial \phi) \omega^2 \cos \alpha / m \quad (17)$$

$$\begin{aligned} G_{21} &= \left(\rho V^2 Sc / 2m I_{yy} \right) \left(C_M^{\delta_e} - C_L^{\delta_e} C_M^{\delta_c} / C_L^{\delta_c} \right) \\ &\quad [\cos \gamma ((\partial T / \partial \alpha) \sin \alpha + T \cos \alpha + \partial L / \partial \alpha) \\ &\quad + c_e \sin \gamma ((\partial T / \partial \alpha) \cos \alpha - T \sin \alpha - \partial D / \partial \alpha)] \end{aligned} \quad (18)$$

$$G_{22} = (\partial T / \partial \phi) \omega^2 \sin(\alpha + \gamma) / m \quad (19)$$

where $\mathbf{x} = [V \ \gamma \ \alpha \ \phi \ h]^T$ and $\ddot{\mathbf{x}}_0 = [\ddot{V} \ \ddot{\gamma} \ \ddot{\alpha} \ \ddot{\phi} \ \ddot{h}]^T$. Then (13) can be written as:

$$\begin{bmatrix} \dot{S}_1 \\ \dot{S}_2 \end{bmatrix} = \begin{bmatrix} f_v + \sum_{i=0}^2 C_3^{2-i} \lambda_1^{i+1} e_v^{(2-i)} - \ddot{V}_c \\ f_h + \sum_{j=0}^3 C_4^{3-j} \lambda_2^{j+1} e_h^{(3-j)} - h_c^{(4)} \end{bmatrix} + \mathbf{G} \cdot \mathbf{u} \quad (20)$$

where

$$\mathbf{u} = \begin{bmatrix} \delta_e \\ \phi_c \end{bmatrix}, \quad \mathbf{G} = \begin{bmatrix} G_{11} & G_{12} \\ G_{21} & G_{22} \end{bmatrix}$$

C. Sliding Mode Controller Design

With the form of equation (20), the sliding controller is then designed to drive the derivatives of the sliding surfaces to satisfy the following forms:

$$\begin{bmatrix} \dot{S}_1 \\ \dot{S}_2 \end{bmatrix} = \begin{bmatrix} -k_1 \text{sat}(S_1 / \Theta_1) - k_2 S_1 \\ -k_3 \text{sat}(S_2 / \Theta_2) - k_4 S_2 \end{bmatrix} \quad (21)$$

where k_i ($i = 1, \dots, 4$) and Θ_1, Θ_2 are strictly positive constants.

Combining (20) and (21), we can get

$$\mathbf{u} = \begin{bmatrix} G_{11} & G_{12} \\ G_{21} & G_{22} \end{bmatrix}^{-1} \begin{bmatrix} \ddot{V}_c - \sum_{i=0}^2 C_3^{2-i} \lambda_1^{i+1} e_v^{(2-i)} - f_v - u_v \\ h_c^{(4)} - \sum_{j=0}^3 C_4^{3-j} \lambda_2^{j+1} e_h^{(3-j)} - f_h - u_h \end{bmatrix} \quad (22)$$

where $u_v = k_1 \text{sat}(S_1 / \Theta_1) + k_2 S_1$, $u_h = k_3 \text{sat}(S_2 / \Theta_2) + k_4 S_2$.

D. Interval Type-2 Fuzzy Sliding Mode Controller Design

In the real-time dynamics, there are uncertainties which cannot be easily obtained from both sensors and FAHV flexible modes. Moreover, due to those uncertainties and interferences of the FAHV model, calculation values f_v and f_h in (14) and (15) may not reflect the accurate dynamic conditions and would make negative contributions to robustness of the control system. As T2-FLSs and IT2-FLSs have the potential to perform better than T1-FLSs and both T1-FLS and IT2-FLS are universal approximator [16, 17], we replace f_v and f_h with uncertainty-embedded approximation values \hat{f}_v and \hat{f}_h . Then (22) can be expressed as:

$$\begin{bmatrix} \delta_e \\ \phi_c \end{bmatrix} = \mathbf{G}^{-1} \begin{bmatrix} \ddot{V}_c - \sum_{i=0}^2 C_3^{2-i} \lambda_1^{i+1} e_v^{(2-i)} - \hat{f}_v - u_v \\ h_c^{(4)} - \sum_{j=0}^3 C_4^{3-j} \lambda_2^{j+1} e_h^{(3-j)} - \hat{f}_h - u_h \end{bmatrix} \quad (23)$$

where \hat{f}_v and \hat{f}_h are generated from a Mamdani fuzzy rule based IT2-FLS.

The IT2-FLS consists of a collection of IF-THEN rules in the following form:

Ruleⁱ : If x_v is \widetilde{M}_v^i and x_h is \widetilde{M}_h^i
then Ψf_v is \widetilde{N}_v^i and Ψf_h is \widetilde{N}_h^i

where $i=1,2,\dots,m$. m is the number of rules, $x_v = e_v$, $x_h = e_h$.
The antecedent sets \widetilde{M}_v^i , \widetilde{M}_h^i which have 5 rules separately
are IT2-FSs, and consequent sets \widetilde{N}_v^i , \widetilde{N}_h^i are T1-FSs. The
firing set $\mathcal{F}^i(x)$ and degree of firing f^i associated with the
 i^{th} rule ($i=1,2,\dots,m$) are

$$\mathcal{F}^i(x) = \mu_{\widetilde{M}_v^i}(x_v)\mu_{\widetilde{M}_h^i}(x_h) = [\underline{f}^i, \overline{f}^i] \quad (24)$$

where $\underline{f}^i = \mu_{\widetilde{M}_v^i}(x_v)\mu_{\widetilde{M}_h^i}(x_h)$ and $\overline{f}^i = \bar{\mu}_{\widetilde{M}_v^i}(x_v)\bar{\mu}_{\widetilde{M}_h^i}(x_h)$. The
 $\mu_{\widetilde{M}_l^i}(x_l)$ and $\bar{\mu}_{\widetilde{M}_l^i}(x_l)$ are LMF and UMF grades of $\mu_{\widetilde{M}_l^i}(x_l)$
respectively ($l=v, h$). Assume Z_v^i and Z_h^i are the centroid of
the i^{th} consequent set \widetilde{N}_v^i and \widetilde{N}_h^i respectively, $z_v^i \in Z_v^i, z_h^i \in Z_h^i$.
By using the singleton fuzzification, product inference, center-
average defuzzification, and the center-of-sets type reducer, the
IT2-FLS type-reducer is given by [18]

$$\Psi f_{v\cos} = \int_{z_v^1} \cdots \int_{z_v^m} \int_{f^1} \cdots \int_{f^m} 1 / \sqrt{\sum_{i=1}^m f^i z_v^i} = [\Psi f_{vl}, \Psi f_{vr}] \quad (25)$$

$$\Psi f_{h\cos} = \int_{z_h^1} \cdots \int_{z_h^m} \int_{f^1} \cdots \int_{f^m} 1 / \sqrt{\sum_{i=1}^m f^i z_h^i} = [\Psi f_{hl}, \Psi f_{hr}] \quad (26)$$

where f^i, Z_v^i, Z_h^i are T1-FSs in IT2-FLS.

We use new symbols θ and ξ to denote

$$\theta_\vartheta = (\theta_\vartheta^1, \theta_\vartheta^2, \dots, \theta_\vartheta^m)^T = (z_\vartheta^1, z_\vartheta^2, \dots, z_\vartheta^m)^T = z_\vartheta \quad (27)$$

$$\xi_{\vartheta\xi}^i = f_{\vartheta\xi}^i / \sum_{i=1}^m f_{\vartheta\xi}^i \quad (28)$$

where ϑ represents v and h , ξ represents l and r respectively.
 $\xi_{\vartheta\xi}^i$ denotes the firing values which are used to compute the
boundaries $\Psi f_{\vartheta\xi}$ in (25) (26) and can be obtained by using the
Karnik-Mendel iterative method [19]. Based on IT2-FLS
theory, the uncertainty terms \hat{f}_v and \hat{f}_h in (23) can be
achieved by

$$\begin{cases} \hat{f}_v = (\Psi f_{vl} + \Psi f_{vr})/2 = \theta_v^T (\xi_{vl} + \xi_{vr})/2 \\ \hat{f}_h = (\Psi f_{hl} + \Psi f_{hr})/2 = \theta_h^T (\xi_{hl} + \xi_{hr})/2 \end{cases} \quad (29)$$

E. TD and NSO Design

In IT2-FSMC, high-order derivatives of the velocity and
the altitude are needed in (22) with both real and tracking
commands. However, it is difficult to obtain the high-order
signals. This paper uses tracking differentiator (TD) and
nonlinear state observer (NSO) to estimate the exact flight
states and their high derivatives online.

1) Tracking Differentiator Design

Discrete TD algorithms are implemented as follows [20]:

Velocity channel:

$$\begin{cases} fs_1(N) = -\lambda(\lambda(\lambda(V_c(N) - V_r) + 3\dot{V}_c(N)) + 3\ddot{V}_c(N)) \\ V_c(N+1) = V_c(N) + \tau * \dot{V}(N) \\ \dot{V}_c(N+1) = \dot{V}(N) + \tau * \ddot{V}_c(N) \\ \ddot{V}_c(N+1) = \ddot{V}_c(N) + \tau * fs_1(N) \end{cases} \quad (30)$$

Altitude channel:

$$\begin{cases} fs_2(N) = -\lambda(\lambda(\lambda(h_c(N) - h_r) + 4\dot{h}_c(N)) + 6\ddot{h}_c(N)) + 4\dddot{h}_c(N) \\ h_c(N+1) = h_c(N) + \tau * \dot{h}_c(N) \\ \dot{h}_c(N+1) = \dot{h}_c(N) + \tau * \ddot{h}_c(N) \\ \ddot{h}_c(N+1) = \ddot{h}_c(N) + \tau * \dddot{h}_c(N) \\ \dddot{h}_c(N+1) = \dddot{h}_c(N) + \tau * fs_2(N) \end{cases} \quad (31)$$

where λ is the “velocity factor” which can decide the speed
of the arranged process, and τ is the “time step” which can
determine the length of calculation step size. K is the number
of iteration.

2) Nonlinear State Observer Design

We use NSO to estimate the exact flight states and their
high derivatives online. Discrete NSO algorithms are
implemented as follows [20]:

Velocity channel:

$$\begin{cases} e_1 = q_{11}(N) - V \\ q_{11}(N+1) = q_{11}(N) + \tau * (z_{12}(K) - \mu_{11} * e_1) \\ q_{12}(N+1) = q_{12}(N) + \tau * (q_{13}(K) - \mu_{12} * fal(e_1, 0.5, \tau)) \\ q_{13}(N+1) = q_{13}(N) + \tau * (-\mu_{13} * fal(e_1, 0.25, \tau) + v_{adjust} * U_1) \end{cases} \quad (32)$$

Altitude channel:

$$\begin{cases} e_2 = q_{21}(N) - h \\ q_{21}(N+1) = q_{21}(N) + \tau * (q_{22}(N) - \mu_{21} * e_2) \\ q_{22}(N+1) = q_{22}(N) + \tau * (q_{23}(N) - \mu_{22} * fal(e_2, 0.5, \tau)) \\ q_{23}(N+1) = q_{23}(N) + \tau * (q_{24}(N) - \mu_{23} * fal(e_2, 0.25, \tau)) \\ q_{24}(N+1) = q_{24}(N) + \tau * (-\mu_{24} * fal(e_2, 0.125, \tau) + h_{adjust} * U_2) \end{cases} \quad (33)$$

where $\mu_{11}, \mu_{12}, \mu_{13}$ and $\mu_{21}, \mu_{22}, \mu_{23}, \mu_{24}$ are the “tracking
coefficients” which determine observer performance and τ is
the “time step” which decides the length of calculation step
size. Parameters q_{11}, q_{12}, q_{13} and $q_{21}, q_{22}, q_{23}, q_{24}$ represent
 V, \dot{V}, \ddot{V} and $h, \dot{h}, \ddot{h}, \dddot{h}$ respectively. $U_1 = G_{11}\delta_e + G_{12}\phi_c$ and
 $U_2 = G_{21}\delta_e + G_{22}\phi_c$.

IV. ADAPTIVE LAW AND STABILITY ANALYSIS

In order to adjust parameters included in the IT2-FLS, we
design adaptive laws with optimal parameter estimations
 θ_v^* and θ_h^* :

$$\theta_v^* = \arg \min_{\theta_v \in \Omega_{\theta_v}} \left\{ \sup_{V \in U_v} |f_v - \hat{f}_v| \right\} \quad (34)$$

$$\theta_h^* = \arg \min_{\theta_h \in \Omega_{\theta_h}} \left\{ \sup_{h \in U_h} \left| f_h - \hat{f}_h \right| \right\} \quad (35)$$

where Ω_{θ_v} and Ω_{θ_h} are constraint sets which are defined as:

$$\Omega_{\theta_v} = \left\{ \theta_v \in R^m \mid 0 < |\theta_v| \leq M_v \right\} \quad (36)$$

$$\Omega_{\theta_h} = \left\{ \theta_h \in R^m \mid 0 < |\theta_h| \leq M_h \right\}$$

where M_v and M_h are positive constants. Then the minimum of the approximation error is defined as:

$$\omega = [\omega_v \ \omega_h]^T = [f_v - \hat{f}_v^* \ f_h - \hat{f}_h^*]^T \quad (37)$$

The first-order derivatives of the sliding surfaces can be expressed as:

$$\begin{bmatrix} \dot{S}_1 \\ \dot{S}_2 \end{bmatrix} = \begin{bmatrix} \sum_{i=0}^2 C_3^{2-i} \lambda_1^{i+1} e_v^{(2-i)} + f_v - \ddot{V}_c \\ \sum_{j=0}^3 C_4^{3-j} \lambda_2^{j+1} e_h^{(3-j)} + f_h - h_c^{(4)} \end{bmatrix} + G \begin{bmatrix} \delta_e \\ \phi_c \end{bmatrix} \quad (38)$$

Replacing the vector $[\delta_e \ \phi_c]^T$ with (23), then (38) can be written as:

$$\begin{aligned} \begin{bmatrix} \dot{S}_1 \\ \dot{S}_2 \end{bmatrix} &= \begin{bmatrix} f_v - \hat{f}_v - u_v \\ f_h - \hat{f}_h - u_h \end{bmatrix} \\ &= \begin{bmatrix} \hat{f}_v^* - \hat{f}_v - u_v \\ \hat{f}_h^* - \hat{f}_h - u_h \end{bmatrix} + \omega \\ &= \begin{bmatrix} \phi_v^T (\xi_{vl} + \xi_{vr}) / 2 - u_v \\ \phi_h^T (\xi_{hl} + \xi_{hr}) / 2 - u_h \end{bmatrix} + \omega \end{aligned} \quad (39)$$

where $\phi_v = \theta_v^* - \theta_v$, $\phi_h = \theta_h^* - \theta_h$. $C_3^{2-i} \lambda_1^{i+1}$, $C_4^{3-j} \lambda_2^{j+1}$ ($i=0, 1, 2$; $j=0, 1, 2, 3$) are Hurwitz polynomial coefficients.

The Lyapunov function candidate is chosen as (40) in order to analyze the system's close-loop stability.

$$V = \frac{1}{2} S^T S + \frac{1}{2\gamma_1} \phi_v^T \phi_v + \frac{1}{2\gamma_2} \phi_h^T \phi_h \quad (40)$$

Differentiating equation (40), we get

$$\begin{aligned} \dot{V} &= S^T \dot{S} + \phi_v^T \dot{\phi}_v / \gamma_1 + \phi_h^T \dot{\phi}_h / \gamma_2 \\ &= \phi_v^T (2\dot{\phi}_{vl} + \gamma_1 S_1 (\xi_{vl} + \xi_{vr})) / 2\gamma_1 \\ &\quad + \phi_h^T (2\dot{\phi}_{hl} + \gamma_2 S_2 (\xi_{hl} + \xi_{hr})) / 2\gamma_2 + S^T (\omega - [u_v \ u_h]^T) \end{aligned} \quad (41)$$

Based on (41), we can design the adaptive law as:

$$\begin{cases} \dot{\theta}_v = \gamma_1 S_1 (\xi_{vl} + \xi_{vr}) / 2 \\ \dot{\theta}_h = \gamma_2 S_2 (\xi_{hl} + \xi_{hr}) / 2 \end{cases} \quad (42)$$

where $\dot{\phi}_v = -\dot{\theta}_v$, $\dot{\phi}_h = -\dot{\theta}_h$.

Substituting (42) to (41), we have

$$\begin{aligned} \dot{V} &= S^T (\omega - [u_v \ u_h]^T) \\ &= S^T \omega - k_{11} S_1 \text{sat}(S_1) - k_{12} S_1^2 - k_{21} S_2 \text{sat}(S_2) - k_{22} S_2^2 \\ &\leq S^T \omega - k_{11} |S_1| - k_{12} S_1^2 - k_{21} |S_2| - k_{22} S_2^2 \end{aligned} \quad (43)$$

When ω is small enough and k_{ij} ($i, j = 1, 2$) are strictly positive constants, we can guarantee the absolute values of the sliding surfaces and tracking errors converge to zero.

V. SIMULATION

To verify the effectiveness of the proposed controller, four cases are studied with different levels of parameter uncertainties with a sliding mode controller (SMC), the adaptive interval type-2 fuzzy sliding mode controller (IT2-FSMC) and adaptive type-1 fuzzy sliding mode controller (T1-FSMC) which adopts simplified type-1 membership functions to replace the type-2 ones in IT2-FSMC for making comparisons with each other. All parameters are set in Table I. The step command signals are set as 4000 feet and 300feet/s in altitude and velocity channels, respectively. The parameter uncertainties of L, T, D, M in (7) are chosen as 0%, 10%, 20% and 30%. The drag D adds positive levels of uncertainties where the other three add negative levels of uncertainties.

TABLE I. CONTROL PARAMETERS

Parameter	Value	Parameter	Value
λ (TD velocity)	0.5	k_{ec}	-0.79639
λ (TD altitude)	0.2	$\mu_{11, 12, 13}$	150, 500, 3500
$\lambda_{1,2}$	2.35, 1.05	$\mu_{21, 22, 23, 24}$	180, 300, 1500, 2200
$k_{1, 2, 3, 4}$	6, 11, 5.5, 10.5	$\Theta_{1, 2}$	1.5, 2

A. Without Parameter Uncertainties

Since the estimation values \hat{f}_v and \hat{f}_h from IT2-FLS are mainly used to replace the computational values of f_v , f_h and uncertainties, in this case all of the three controllers can make the system stably controlled in tracking reference signals which are generated through arranged tracking process (ATP) (Fig. 3 a), b)). The IT2-FSMC and T1-FSMC perform nearly the same responses under this condition (Fig. 3 and Fig. 4). Furthermore, the improved tracking error convergences (Fig. 3 c), d)) and flexible mode suppression performances of η_1 (Fig. 4 c)) in these two fuzzy sliding mode controllers are better than the sliding mode controller.

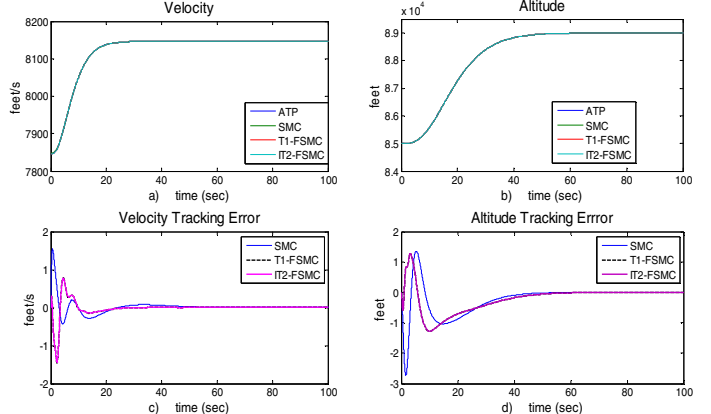


Fig. 3 System Responses in velocity and altitude channels

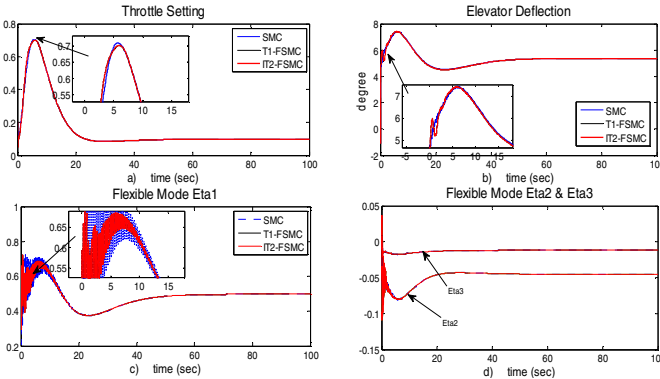


Fig. 4 System Responses in actuators and flexible modes

B. With 10%~30% Parameter Uncertainties

All these three controllers show strong robustness when facing parameter uncertainties from 10% up to 30%. With the growing level of uncertainties, the control abilities among the three controllers have a certain decline respectively. Moreover, Fig. 5 a) to f) demonstrate that IT2-FSMC has the strongest robustness than T1-FSMC and SMC in both convergence time and tracking errors. In addition, the simulation results show that the velocity channel is more sensitive than the altitude channel when using different controllers.

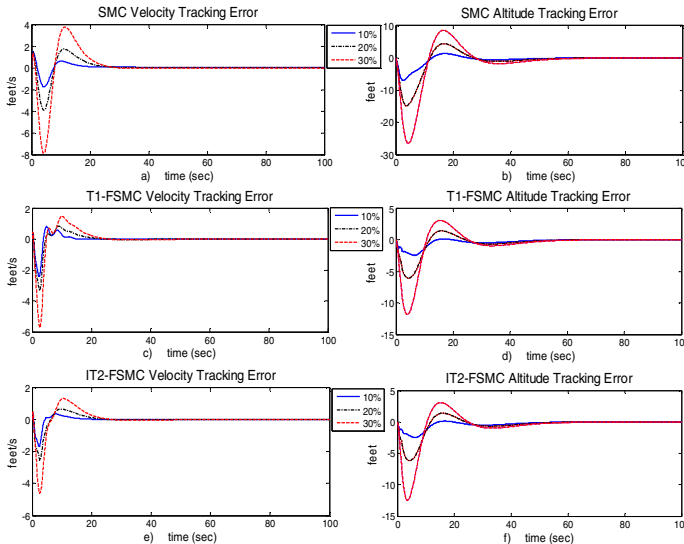


Fig. 5 System Responses with 10%, 20% and 30% Uncertainties

VI. CONCLUSIONS

The promising development of the flexible air-breathing hypersonic vehicle faces numerous challenges which include the uncertainties brought by flexible effects and high aerodynamic coupling, etc. Based on the Lyapunov synthesis approach, the proposed control system can achieve asymptotic stability and the adaptive parameters in the adaptive interval type-2 fuzzy sliding mode controller (IT2-FSMC) can be tuned on-line by adaptive laws. Furthermore, the simulation comparison studies show better robustness and effectiveness of the proposed adaptive IT2-FSMC in dealing with different

levels of uncertainties than adaptive type-1 fuzzy sliding mode controller and sliding mode controller.

REFERENCES

- [1] J. D. Shaughnessy, S. Z. Pinckney, and J. D. McMinn, *Hypersonic vehicle simulation model Winged-cone configuration*: National Aeronautics and Space Administration, Langley Research Center, 1990.
- [2] P. Tartabini, D. Bose, M. Thornblom, J. Lien, and J. Martin, "Mach 10 Stage Separation Analysis for the X43-A," presented at the 44th AIAA Aerospace Sciences Meeting and Exhibit, Reno, Nevada, 2006.
- [3] J. Hank, J. Murphy, and R. Mutzman, "The X-51A Scramjet Engine Flight Demonstration Program," in *15th AIAA International Space Planes and Hypersonic Systems and Technologies Conference*, Dayton, Ohio, 2008.
- [4] A. Levant, "Higher-order sliding modes, differentiation and output-feedback control," *International Journal of Control*, vol. 76, pp. 924-941, 2003.
- [5] T. Niknam, M. H. Khooban, A. Kavousifard, and M. R. Soltanpour, "An optimal type II fuzzy sliding mode control design for a class of nonlinear systems," *Nonlinear Dynamics*, vol. 75, pp. 73-83, 2014.
- [6] L. A. Zadeh, "The concept of a linguistic variable and its application to approximate reasoning-I," *Information Sciences*, vol. 8, pp. 199-249, 1975.
- [7] D. Wu and J. M. Mendel, "Designing Practical Interval Type-2 Fuzzy Logic Systems Made Simple," in *2014 IEEE International Conference on Fuzzy Systems*, Beijing, China, 2014, pp. 800-807.
- [8] M.-Y. Hsiao, T.-H. S.Li, J.-Z. Lee, C.-H. Chao, and S.-H. Tsai, "Design of interval type-2 fuzzy sliding-mode controller," *Information Sciences*, vol. 178, pp. 1969-1716, 2008.
- [9] T.-C. Lin and M.-C. Chen, "Hybrid Adaptive Interval Type-2 Fuzzy Sliding Mode Controller for Chaos Synchronization of Uncertain Chaotic Systems," in *2010 International Symposium on Computer Communication Control and Automation (3CA)*, Tainan, 2010.
- [10] M. A. Bolender and D. B. Doman, "A non-linear model for the longitudinal dynamics of a hypersonic air-breathing vehicle," in *AIAA Guidance, Navigation, and Control Conference and Exhibit*, San Francisco, USA, 2005.
- [11] C. Sun, Y. Huang, C. Qian, and L. Wang, "On modeling and control of a flexible air-breathing hypersonic vehicle based on LPV method," *Frontiers of Electrical and Electronic Engineering*, vol. 7, pp. 56-68, 2012.
- [12] F. Yang, J. Yi, X. Tan, and R. Yuan, "Robust Adaptive Type-2 Fuzzy Logic Controller Design for a Flexible Air-breathing Hypersonic Vehicle," in *2014 IEEE International Conference on Fuzzy Systems*, Beijing, China, 2014, pp. 106-112.
- [13] L. Fiorentini, A. Serrani, M. A. Bolender, and D. B. Doman, "Nonlinear Robust Adaptive Control of Flexible Air-Breathing Hypersonic Vehicles," *Journal of Guidance, Control, and Dynamics*, vol. 32, pp. 402-417, 2009.
- [14] L. Fiorentini, "Nonlinear Adaptive Controller Design for Air-breathing Hypersonic Vehicles," Ph.D dissertation, Electrical and Computer Engineering Department, The Ohio State University, 2010.
- [15] H. Xu, M. D. Mirmirani, and P. A. Ioannou, "Adaptive sliding mode control design for a hypersonic flight vehicle," *Journal of Guidance, Control, and Dynamics*, vol. 27, pp. 829-838, 2004.
- [16] H. Ying, "General Interval Type-2 Mamdani Fuzzy Systems Are Universal Approximators," in *Proceedings of North American Fuzzy Information Processing Society Conference*, New York, USA, 2008.
- [17] C. Li, J. Yi, and G. Zhang, "On the Monotonicity of Interval Type-2 Fuzzy Logic Systems," *IEEE Transactions on Fuzzy Systems*, vol. 22, pp. 1197-1212, 2014.
- [18] N. N. Karnik and J. M. Mendel, "Centroid of a type-2 fuzzy set," *Information Sciences*, vol. 132, pp. 195-220, 2001.
- [19] J. M. Mendel, "Type-2 fuzzy sets and systems: an overview," *Computational Intelligence Magazine, IEEE*, vol. 2, pp. 20-29, 2007.
- [20] J. Han, *Active Disturbance Rejection Control Technique*. Beijing: National Defense Industry Press, 2009.